Blackwell
Publishing

Full-length article

Astragaloside IV inhibits spontaneous synaptic transmission and synchronized Ca^{2+} oscillations on hippocampal neurons[1]

Shao-qing ZHU, Lei QI, Yan-fang RUI, Ru-xin LI, Xiang-ping HE, Zuo-ping XIE[2]

Department of Biological Science and Biotechnology, State Key Laboratory of Biomembrane and Membrane Biotechnology, Tsinghua University, Beijing 100084, China

Abstract

Aim: To investigate the changes in the spontaneous neuronal excitability induced by astragaloside IV (AGS-IV) in the cultured hippocampal network. **Methods:** Hippocampal neurons in culture for 9–11 d were used for this study. The spontaneous synaptic activities of these hippocampal neurons were examined by Ca^{2+} imaging and whole-cell patch-clamp techniques. In total, 40 mg/L AGS-IV dissolved in DMSO and 2 mL/L DMSO were applied to the neurons under a microscope while the experiments were taking place. **Results:** AGS-IV inhibited the frequencies of synchronized spontaneous Ca^{2+} oscillations to 59.39%±3.25% (mean±SEM), the spontaneous postsynaptic currents to 43.78%±7.72% (mean±SEM), and the spontaneous excitatory postsynaptic currents to 49.25%±7.06% (mean±SEM) of those of the control periods, respectively, at 16 min after the AGS-IV applications. AGS-IV also decreased the peak values of the voltage-gated K$^+$ and Na$^+$ channel currents at that time point. **Conclusion:** These results indicate that AGS-IV suppresses the spontaneous neuronal excitabilities effectively. Such a modulation of neuronal activity could represent new evidence for AGS-IV as a neuroprotector.

Introduction

Astragalus membranaceus, a traditional Chinese herb, has been reported to have a range of pharmacological effects. Astragaloside IV (AGS-IV; 3-*O*-beta-*D*-xylopyranosyl-6-*O*-beta-*D*-glucopyranosyl-cycloastragenol, molecular structure shown in Figure 1), as the main active ingredient of *Astragalus membranaceus*, is a small molecular weight (MW 784) saponin. Current clinical and laboratory-based research has focused on the effects of AGS-IV with regards to anti-inflammation[1], antioxidation[2], antivirus[3], anti-apoptosis[4], immunomodulation[5], ischemia injury protection[6–8], cardioprotection[6,9], gastroprotection[10], and so on. More research on the cellular mechanisms of AGS-IV will not only contribute to the understanding of the efficacies of *Astragalus membranaceus* for clinical treatment, but would also lead to the development of potential therapeutic strategies for the treatment of relative diseases.

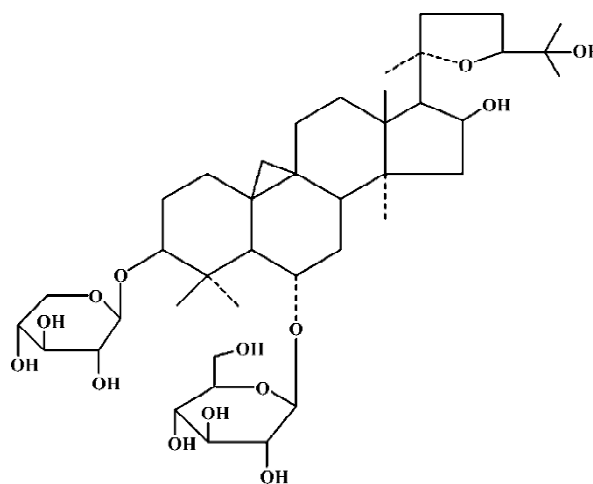The ability of neuronal networks to generate spontaneous firing patterns and to synchronize the activity of many

Figure 1. Chemical structure of AGS-IV.

cells is central to a wide range of processes in the central nervous system, such as the development of neuronal

networks, epileptic activity, and neuronal plasticity[11]. Synchronized spontaneous Ca^{2+} oscillations are mostly the direct result of membrane depolarization from action potentials among synaptically connected neurons[12,13]; they are often observed among networked neurons without external stimuli *in vitro*, resulting from periodic burst firing of action potentials through excitatory synaptic transmissions[12,14], which could be recorded as the form of spontaneous excitatory postsynaptic currents (sEPSC). Some researchers have found that the spontaneous Ca^{2+} oscillation is mainly mediated by non-*N*-methyl-D-aspartate (NMDA)-type glutamatergic transmission[15,16], while others have discovered that the concomitant activation of NMDA receptors and voltage-activated L-type Ca^{2+} channels allows Ca^{2+} entering from the extracellular medium and sustaining the long depolarization, which shapes every single calcium wave[14]. One study suggests that the neuron's spontaneous activity is initiated by an action potential-dependent spontaneous vesicular release of glutamate from presynaptic terminals, depolarizing postsynaptic cells to the action potential threshold[17]. This activity could induce the recordable spontaneous postsynaptic currents (sPSC) and especially the sEPSC *in vitro*. As a result, the synchronized spontaneous Ca^{2+} oscillations, sPSC, and sEPSC indicate the functional transmission between neurons and they both reflect the whole neuronal activity.

It is clear that the ion channels, both voltage- and ligand-gated, underlie the spontaneous activity[18]. In the early 1950s, Hodgkin and Huxley's classic investigations into the components of the squid giant axon action potential recognized that Na^+ influx through voltage-gated channels initializes and propagates the action potentials; K^+ out of the cell produces rapid repolarization of the cell membrane after a depolarizing spike[19]. Presynaptic voltage-gated Na^+ channels are involved in the control of synaptic transmission[20]. Any drug or modulator that increases the opening of a particular K^+ channel can greatly reduce the excitability of the tissue expressing that channel, and the action potential breadth is narrower in part because of greater K^+ efflux triggered by voltage change and changes in intracellular Ca^{2+}[21].

Therefore, the parameters described above will exhibit the spontaneous electrophysiological characteristics of neurons without any stimuli. Here, we uncover the effects of AGS-IV in large populations of neurons from an *in vitro* hippocampus preparation.

Material and methods

Drugs Dulbecco's modified Eagle's medium (DMEM) media, neurobasal medium, fetal bovine serum, B27 supplements, 0.25% trypsin-EDTA, and poly-D-lysine for the cell culture were from Invitrogen (Carlsbad, CA, USA). Equine serum and L-glutamine were from Hyclone (Logan, UT, USA). AGS-IV was purchased from the National Institute for the Control of Pharmaceutical and Biological Products (Beijing, China) and was dissolved in DMSO. Fluo-4-AM was from Molecular Probes (Eugene, OR, USA). The other reagents were purchased from Sigma (St Louis, MO, USA).

Cell culture All of the animal experiments followed the guidelines for the care and use of laboratory animals provided by our institution. Hippocampal neurons from embryonic Sprague-Dawley rats (E18) were obtained according to the method previously described[22]. In brief, hippocampal tissues from 18 d fetal rats were dissected and treated with 0.25% trypsin at 37 °C for 15 min; they were then dissociated by trituration with a glass Pasteur pipette and plated in 35 mm culture dishes with a glass bottom (MatTek, Ashland, MA, USA) for culture and subsequent microscopy. The glass surface in each dish (15 mm diameter) was pretreated with poly-D-lysine for 2 h (500 mg/L in borate buffer), washed 3 times, and air-dried before cell plating. Approximately 25 000 cells were plated in the glass area of each dish in DMEM containing 5% fetal bovine serum, 5% equine serum, and 500 mm glutamine. On the second day after plating, the culture medium was replaced by serum-free neurobasal medium containing the B27 supplement and 500 mm glutamine for reduced glial growth. The cells were maintained in a CO_2 incubator at 37 °C, and one-half volume of the culture medium was replaced with fresh neurobasal medium every 3 d. All the experiments were performed on 9–11 d cultures after plating.

Ca^{2+} imaging The hippocampal cells were loaded with 6 µmol/L Fluo-4-AM, which was dissolved in DMSO in Krebs-Ringer's saline (in mmol/L: 150 NaCl, 5 KCl, 2 $CaCl_2$, 1 $MgCl_2$, 10 glucose, and 10 HEPES (2-[4-(2-Hydroxyethy)-1-piperazinyl]ethanesulfoinc acid), pH 7.4) at 37 °C for 30 min, followed by 3 washes and a 15 min incubation period for the further de-esterification of Fluo-4-AM before imaging. The cells grown on the glass bottom in 35 mm dishes were directly imaged on a Nikon (Tokyo, Japan) inverted microscope (TE 300) using a 40×numerical aperture, 1.30 oil immersion Plan Fluor objective. A Lambda DG-4 high-speed wavelength switcher (Sutter Instruments, Novato, CA, USA) was used for the Fluo-4-AM excitation at 488 nm, and a cooled CCD (Charged coupled device) camera (CoolSnap FX; Roper Scientific, Princeton, NJ, USA) was used for the image acquisition. MetaFluor imaging software (Universal Imaging, Downingtown, PA, USA) was used for hardware control,

imaging acquisition, and image analysis. The hippocampal cells were maintained at 35–37 °C during the imaging through the use of a heater positioned near the microscope stage. Typically, the time-lapse recording of Ca^{2+} signals in hippocampal neurons were performed for 2 min control periods before and an 18 min period after the application of different chemicals; the sampling rate was 1 frame every 2 s with a typical exposure time of 50 ms when the CCD binning of 4×4 was used.

Electrophysiology Synaptic and voltage-gated ion channel currents were recorded from the somatic region of pyramidal-like hippocampal neurons using the whole-cell patch-clamp technique. The culture medium was replaced with extracellular solution (in mmol/L: 140 NaCl, 3 $CaCl_2$, 1 $MgCl_2$, 5 KCl, 10 HEPES, and 10 glucose, pH 7.4). Synaptic sEPSC were isolated by the application of 0.05 mmol/L bicuculline, the light-sensitive competitive antagonist to the $GABA_A$ (GABA: γ-Aminobutyric Acid) receptors in the extracellular solution. The patch pipettes (4–6 MΩ resistance) were filled with an intracellular solution (in mmol/L: 140 KCl, 10 HEPES, and 10 EGTA (O,O'-Bis(2-aminoethyl)ethyleneglycol-*N*,*N*,*N*', *N*'-tetraacetic acid), pH 7.2). Whole-cell patch-clamp recordings were made at room temperature (21–23 °C) with the Axopatch-200B amplifier (Axon Instruments, Foster City, CA, USA) in conjunction with pClamp9 software (Axon Instruments, USA). In the gap-free mode, the cell was clamped at -70 mV without any stimuli. In the episodic mode, the cell was clamped at assumptive resting potential (-70 mV), and step depolarized to +60 mV in 10 mV increments. The signals were filtered with a current filter at 5 kHz.

Quantitative analysis of synchronized Ca^{2+} oscillations The quantitative measurements of changes in intracellular Ca^{2+} concentrations were done by obtaining the average Fluo-4-AM fluorescence intensity of a 3×3 $pixel^2$ analysis box placed at the center of the cell body; the intensity values were then subtracted from the average background intensity measured in the cell-free regions. Changes in the intracellular Ca^{2+} concentration for each cell were then represented by the changes of relative fluo-4 fluorescence (DF/F_0) when F_0 was the baseline intensity obtained from the 2 min control period. The Ca^{2+} oscillations were defined as a rapid elevation of DF/F_0 equal to or >20%. Under our imaging settings, fields of 3–10 neurons were typically recorded and subsequently analyzed. To determine the frequency of Ca^{2+} oscillations, we counted the number of Ca^{2+} oscillations over a 2 min period of the recording at a defined time point. To assess the change in the spike frequency, these frequency values after the drug application were normalized to the control frequency and expressed as percentages, with a value of 100% indicating no change.

Quantitative analysis of electrophysiological results Two periods of recording were performed, one before and one after the addition of drugs. We typically used the changes over every 2 min after the application for assessing the effects of a particular molecule on the spike frequency and the changes of the whole-cell K^+ and Na^+ currents 16 min after the drug application. The quantitative analyses of the sPSC and sEPSC were the same as the calcium imaging: the frequency values recorded every 2 min after the drug application were normalized to the control frequency and expressed as percentages, with a value of 100% indicating no change. The peak values of voltage-gated K^+ and Na^+ currents were analyzed separately by Clampfit 9 software (Axon Instruments, USA). Data from the dishes of different batches of cultures were pooled together and analyzed for statistical significant differences using a paired *t*-test. Compiled data are expressed and graphed as mean±SEM, with *n* denoting the number of neurons studied.

Results

AGS-IV decreased the frequency of synchronized spontaneous Ca^{2+} oscillations To examine the effects of AGS-IV on synchronized Ca^{2+} oscillations, we bath-applied AGS-IV to hippocampal cultures and performed Ca^{2+} imaging before and after application (Figure 2A). We found that AGS-IV (40 mg/L) dissolved in DMSO could significantly reduce the frequency of synchronized spontaneous Ca^{2+} oscillations (Figure 2B). While the bath application of DMSO that had the same volume as AGS-IV (2 mL/L) did not affect the spike frequency (Figure 2C), it indicated that no artifact was produced by the bath application method and the inhibitive effect on Ca^{2+} oscillations was not because of DMSO. To quantify the frequency change of AGS-IV on Ca^{2+} oscillations, we determined the spike frequency at various time points after AGS-IV application and compared it to that of the control period. The results of the t-test showed that at 6 min after AGS-IV application, there appeared to be an obvious change in the frequency of Ca^{2+} oscillations compared with that in the DMSO group (Figure 2D). At the same time, we found that at 16 min after AGS-IV application, the spike frequency decreased to 59.39%±3.25% (mean±SEM).

AGS-IV inhibited spontaneous postsynaptic transmission We also performed electrophysiological recordings using the whole-cell patch-clamp method. Consistent with previously reported studies[23,24], our cultures contained an enriched population of pyramidal glutamatergic neurons, whereas a low percentage of inhibitory GABAergic cells could be found. The hippocampal neurons exhibited peri-
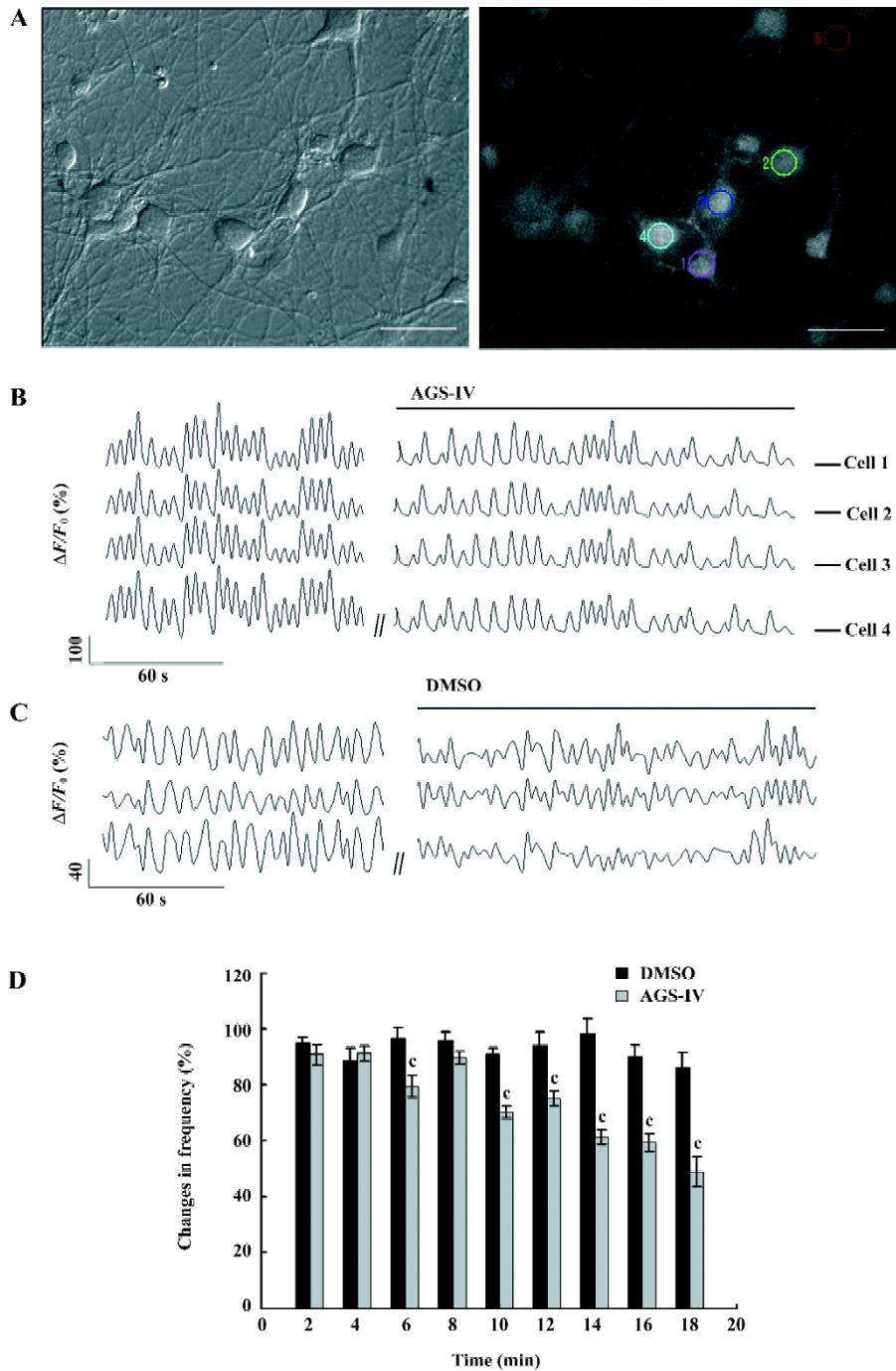
Figure 2. AGS-IV decreased the frequency of synchronized Ca^{2+} spike firing. (A) The digital interface controller (DIC) image on the left shows interconnected hippocampal neurons. Fluorescent image on the right shows the same region of hippocampal neurons with the DIC image loaded with Fluo-4. Scale bar: 40 mm. (B) traces show synchronized Ca^{2+} oscillations in the 4 neurons randomly selected from this group of synchronically firing cells before and after the bath addition of AGS-IV (final 40 mg/L). (C) traces show synchronized Ca^{2+} oscillations in the 3 neurons randomly selected from a group of synchronically firing cells before and after the bath addition of DMSO (final 2 mL/L, the same volume as AGS-IV). The time gaps (//) at both B and C are 16 min. (D) changes of the Ca^{2+} spike frequency every 2 min after DMSO and AGS-IV applications. Change of the Ca^{2+} spike frequency was quantified by normalizing the spike number from every 2 min period after the bath application to the spike number in the control. Data are presented as the mean±SEM from many cells (DSMO: $n=20$; AGS-IV: $n=14$). [c]$P<0.01$ *vs* DMSO control.

odic firing that was recorded as sPSC, which contained sEPSC and spontaneous inhibitory postsynaptic currents (IPSC). Moreover, the sEPSC caused by excitatory glutamatergic synaptic transmissions corresponded to Ca^{2+} oscillations. The application of 40 mg/L AGS-IV significantly decreased the frequency of the sPSC (Figure 3B) and sEPSC (Figure 4B), while there was no difference in the frequency in the DMSO group (Figures 3A,4 A), respectively. We quantified the frequency of spontaneous firing by counting the number of sPSC and sEPSC every 2 min and then compared it to that of the control period. The results of the t-test showed that there were obvious discrepancies in the frequency of sPSC and sEPSC from 6 min after AGS-IV application compared with their DMSO groups, respectively. We found that

at 16 min after AGS-IV application, the spontaneous neuronal firing decreased to 43.78%±7.72% (mean±SEM; Figure 3C), and the frequency of the sEPSC decreased to 49.25%±7.06% (mean±SEM; Figure 4C). These findings were almost consistent with the inhibitive effect of AGS-IV on the frequency of Ca^{2+} oscillations resulting from the excitatory action potentials of hippocampal networks in culture.

AGS-IV repressed voltage-gated K^+ and Na^+ currents of
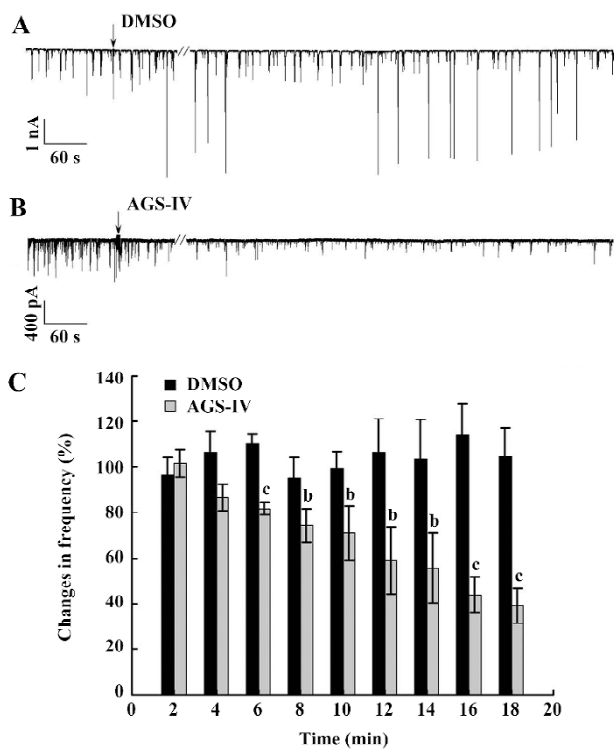

Figure 3. AGS-IV decreased the frequency of the spontaneous firing of hippocampal neurons, as recorded by the whole-cell patch–clamp technique. (A) effects of DMSO on sPSC in a hippocampal neuron from a 9 d culture. Trace represents the sPSC of a hippocampal neuron before and 16 min after the application of DMSO (final 2 mL/L, the same volume as AGS-IV). (B) Effects of AGS-IV on sPSC in a hippocampal neuron from a 9 d culture. Trace represents the sPSC of a hippocampal neuron before and 16 min after the application of AGS-IV (final 40 mg/L). (C) changes in the number of sPSC after DMSO and AGS-IV additions, quantified by normalized sPSC numbers to the number in the control period. Data represent mean±SEM from many cells (DSMO: *n*=6; AGS-IV: *n*=6). [b]*P*<0.05, [c]*P*<0.01 *vs* DMSO control.
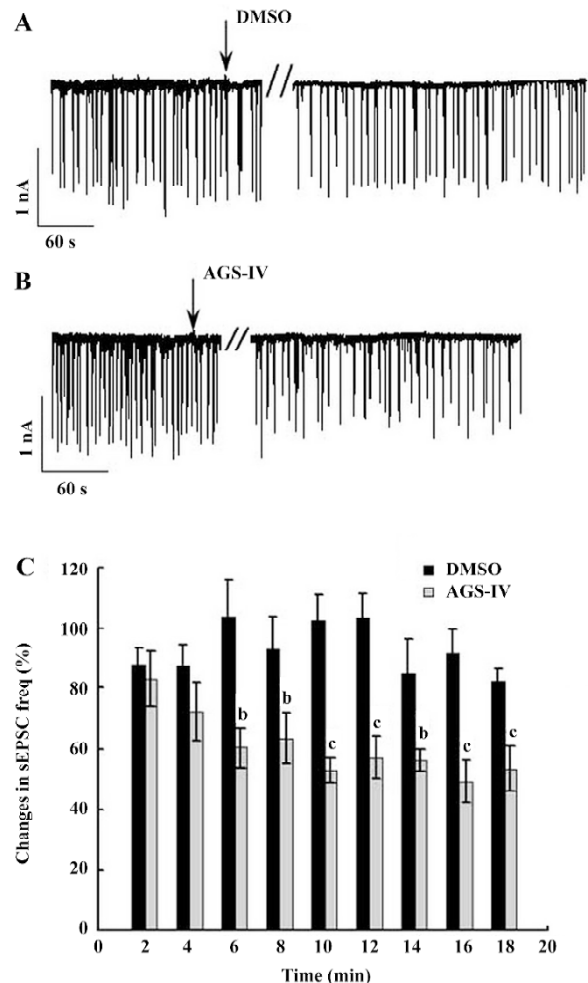
Figure 4. AGS-IV depressed the frequency of spontaneous EPSC. (A) effects of DMSO on sEPSC in a hippocampal neuron from a 9 d culture. Trace represents the sEPSC of a hippocampal neuron before and 16 min after the application of DMSO (final 2 mL/L, the same volume as AGS-IV). (B) effects of AGS-IV on sEPSC in a hippocampal neuron from a 9 d culture. Trace represents the sEPSC of a hippocampal neuron before and 16 min after the application of AGS-IV (final 40 mg/L). (C) changes in the number of sEPSC after DMSO and AGS-IV additions were quantified by normalized sEPSC numbers to the number in the control period. Data represent mean±SEM from many cells (DSMO: *n*=6; AGS-IV: *n*=7). [b]*P*<0.05, [c]*P*<0.01 *vs* DMSO control.
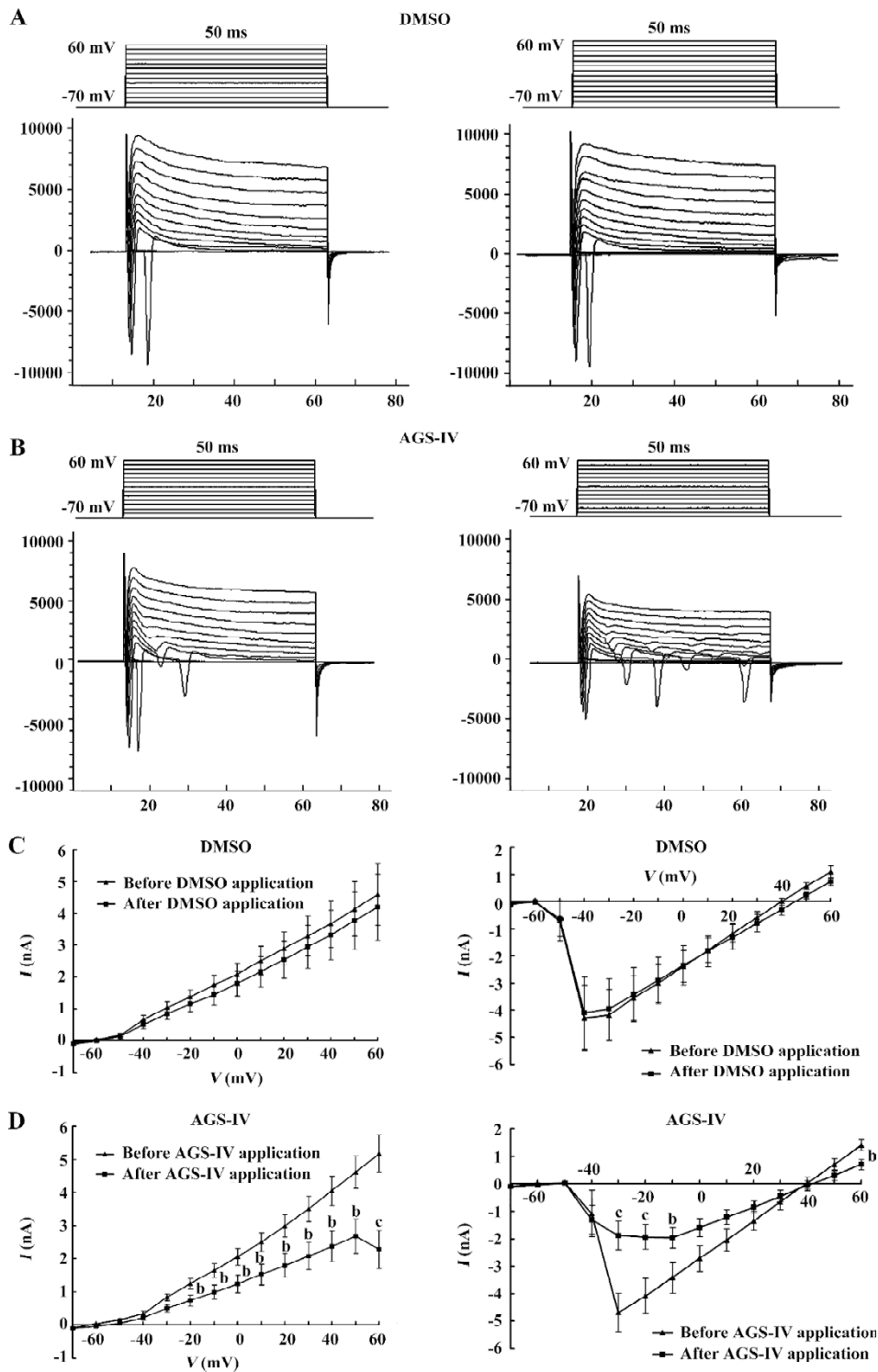
Figure 5. AGS-IV inhibited the currents of voltage-gated K^+ and Na^+ channels. (A) an example of K^+ and Na^+ currents recorded from a cultured hippocampal neuron before (left) and 16 min after (right) DMSO application. (B) an example of K^+ and Na^+ currents recorded from a cultured hippocampal neuron before (left) and 16 min after (right) AGS-IV addition. (C) The *I–V* curve shows that there are no obvious changes in voltage-gated K^+ (left) and Na^+ (right) current 16 min after DMSO application. (D) *I–V* curve shows that there are significant decreases of K^+ current 16 min after AGS-IV application at the voltage from -20 mV to +60 mV (left) and Na^+ current at -30 mV, -20 mV, -10 mV, and +60 mV (right). Data represent mean±SEM from many cells (DSMO: *n*=9; AGS-IV: *n*=10). [b]$P<0.05$, [c]$P<0.01$ *vs* DMSO control.

cultured rat hippocampal neurons To test the effects of AGS-IV on the whole-cell voltage-gated K^+ and Na^+ currents, we applied AGS-IV to hippocampal cultures and performed electrophysiology before and after drug application. Since there were significant effects of AGS-IV on the frequencies of both Ca^{2+} oscillations and sPSC after 16 min compared with their control periods, respectively, we chose that time point to record the K^+ and Na^+ currents after the DMSO and AGS-IV additions (Figure 5A, 5B). We found that AGS-IV induced marked decreases in the peak values of the Na^+ currents at -30 mV, -20 mV, -10 mV, and +60 mV compared with those before the AGS-IV applications (Figure 5D). At the same time, AGS-IV reduced the peak values of the K^+ currents at the stimuli from -20 mV to +60 mV (Figure 5D), but DMSO had no influence (Figure 5C). These data suggested that AGS-IV not only suppressed spontaneous neuronal activity, but also changed the peak values of voltage-gated K^+ and Na^+ currents.

Discussion

AGS-IV, the main functional ingredient of the Chinese herb Astragalus membranaceus, has many pharmacological functions. Although AGS-IV has a neuroprotective effect in the model of ischemic brain injury[7] and has anti-apoptosis action[4,25], there is almost no immediate evidence to demonstrate the cellular mechanism of AGS-IV on the protective effect of neurons. Since the spontaneous discharge of cultured primary hippocampal neurons is a widely studied model of physiological and pathological neuronal networks *in vitro*, our research made use of this model and discovered that AGS-IV not only inhibited the neuronal spontaneous excitabilities through suppressing the excitatory synaptic transmission and synchronic Ca^{2+} oscillations, but also reduced the peak values of voltage-gated K^+ and Na^+ channels of hippocampal neurons.

AGS-IV decreases the peak value of voltage-gated Na^+ currents in hippocampal neurons, and the frequency of Ca^{2+} oscillation is inhibited in the presence of 40 mg/L AGS-IV by approximately 59%, which is compatible with the suppression of sEPSC. One explanation for the inhibitive effects of AGS-IV on overall membrane excitability is the suppression of voltage-gated Na^+ currents; it then induced an inhibition of Ca^{2+} currents at presynaptic terminals, producing a subsequent reduction of Ca^{2+}-dependent excitatory transmitter release. Since Tetrodotoxin (TTX) could obviously block the synchronized spontaneous Ca^{2+} spikes in cultured hippocampal neurons[13] and inhibited all spontaneously-occurring EPSC and IPSC[26], it is possible that the decrease of TTX-sensitive voltage-gated Na^+ channel currents play a

critical role in the inhibitive effect of AGS-IV. Moreover, AGS-IV inhibits synchronized spontaneous Ca^{2+} oscillation, sPSC, and sEPSC, all of which are tightly relative with neuronal depolarization caused by voltage-gated Na^+ channels.

AGS-IV decreases voltage-gated K^+ currents in cultured hippocampal cells by approximately 55.9% at +60 mV. An inhibition of K^+ channels would tend to increase neuronal excitability and possibly enhance synaptic transmission. This however is in contrast to the depressant effect on the spontaneous hippocampal activity observed with AGS-IV. As a result, we speculate that the increased effect induced through voltage-gated K^+ channels cannot exceed the inhibitive result caused through other factors. Furthermore, the inhibitive effects of AGS-IV on voltage-gated K^+ channel currents may also increase the neuronal excitability through shortening the interval of depolarization and hence induce the larger second and third openings of Na^+ channel during 50 ms stimuli (Figure 5B).

In addition, AGS-IV has very low permeability in caco-2 cells[27], and its absorption is highly sensitive to the extracellular Ca^{2+} concentration[28]. In our study, the obvious effects on the hippocampal neurons appeared almost 10 min after the AGS-IV application. This suggests that the long acting time was caused by the low permeability of AGS-IV and through the extracellular Ca^{2+}-dependent pathway.

There is some research on the protective effects of AGS-IV on ischemic injury in the myocardium and neurons[6–8]. Brain ischemia-induced neuronal death has been linked in part to excess Ca^{2+} influx through ionotropic glutamate receptors and voltage-gated Ca^{2+} channels[29,30]. As a result, considerable effort has been directed towards reducing neuronal circuit excitation as a strategy for neuroprotective intervention. Besides directly blocking the NMDA and AMPA (α-amino-3-hydroxy-5-methylisoxazole-4-propionate) glutamate receptors, additional strategies, including enhancing synaptic inhibition, reducing glutamate release, and reducing neuronal firing by blocking Na^+ have been tested[31–33]. Since in our research AGS-IV inhibited the neuronal excitation of hippocampal neurons through decreasing spontaneous synchronized Ca^{2+} oscillations, the frequency of sPSC, and the voltage-gated Na^+ currents, these data suggest that AGS-IV is a potential drug for the treatment of ischemia-induced neuronal damage.

In summary, our results suggest that AGS-IV inhibits the excitability in cultured hippocampal neurons through the inhibition of synaptic transmission and Ca^{2+} oscillations, and the blockade of voltage-gated K^+ and Na^+ currents. These observations confirm and extend previous findings. For the first time, the effects of AGS-IV have been researched at the cellular level in neuronal networks. Moreover, these data

could help people further understand the traditional meditative mechanism of AGS-IV and accordingly develop new treatments for other diseases.

References

1　Zhang WJ, Hufnagl P, Binder BR, Wojta J. Antiinflammatory activity of astragaloside IV is mediated by inhibition of NF-kappaB activation and adhesion molecule expression. Thromb Haemost 2003; 90: 904–14.

2　Ma Z, Yang Z. Scavenging effects of Astragalus and *Gynostemma pentaphyllum* with its product on O_2 and OH. Zhong Yao Cai 1999; 22: 303–6. Chinese

3　Zhang Y, Zhu H, Huang C, Cui X, Gao Y, Huang Y, *et al*. Astragaloside IV exerts antiviral effects against coxsackievirus B3 by upregulating interferon-gamma. J Cardiovasc Pharmacol 2006; 47: 190–5.

4　Xu ME, Xiao SZ, Sun YH, Ou-Yang Y, Zheng XX. Effects of astragaloside IV on pathogenesis of metabolic syndrome *in vitro*. Acta Pharmacol Sin 2006; 27: 229–36.

5　Wang YP, Li XY, Song CQ, Hu ZB. Effect of astragaloside IV on T, B lymphocyte proliferation and peritoneal macrophage function in mice. Acta Pharmacol Sin 2002; 23: 263–6.

6　Zhang WD, Chen H, Zhang C, Liu RH, Li HL, Chen HZ. Astragaloside IV from *Astragalus membranaceus* shows cardioprotection during myocardial ischemia *in vivo* and *in vitro*. Planta Med 2006; 72: 4–8.

7　Luo Y, Qin Z, Hong Z, Zhang X, Ding D, Fu JH, *et al*. Astragaloside IV protects against ischemic brain injury in a murine model of transient focal ischemia. Neurosci Lett 2004; 363: 218–23.

8　Li ZP, Cao Q. Effects of astragaloside IV on myocardial calcium transport and cardiac function in ischemic rats. Acta Pharmacol Sin 2002; 23: 898–904. Chinese

9　Luo HM, Dai RH, Li Y. Nuclear cardiology study on effective ingredients of Astragalus membranaceus in treating heart failure. Zhongguo Zhong Xi Yi Jie He Za Zhi 1995; 15: 707–9. Chinese

10　Navarrete A, Arrieta J, Terrones L, Abou-Gazar H, Calis I. Gastroprotective effect of Astragaloside IV: role of prostaglandins, sulfhydryls and nitric oxide. J Pharm Pharmacol 2005; 57: 1059–64.

11　Muller TH, Swandulla D, Zeilhofer HU. Synaptic connectivity in cultured hypothalamic neuronal networks. J Neurophysiol 1997; 77: 3218–25.

12　Leinekugel X, Medina I, Khalilov I, Ben-Ari Y, Khazipov R. Ca^{2+} oscillations mediated by the synergistic excitatory actions of GABA(A) and NMDA receptors in the neonatal hippocampus. Neuron 1997; 18: 243–55.

13　Liu Z, Geng L, Li R, He X, Zheng JQ, Xie Z. Frequency modulation of synchronized Ca^{2+} spikes in cultured hippocampal networks through G-protein-coupled receptors. J Neurosci 2003; 23: 4156–63.

14　Bacci A, Verderio C, Pravettoni E, Matteoli M. Synaptic and intrinsic mechanisms shape synchronous oscillations in hippocampal neurons in culture. Eur J Neurosci 1999; 11: 389–97.

15　Tanaka T, Saito H, Matsuki N. Intracellular calcium oscillation in cultured rat hippocampal neurons: a model for glutamatergic neurotransmission. Jpn J Pharmacol 1996; 70: 89–93.

16　Dravid SM, Murray TF. Spontaneous synchronized calcium oscillations in neocortical neurons in the presence of physiological (Mg^{2+}): involvement of AMPA/kainate and metabotropic glutamate receptors. Brain Res 2004; 1006: 8–17.

17　Koller H, Siebler M, Schmalenbach C, Muller HW. GABA and glutamate receptor development of cultured neurons from rat hippocampus, septal region, and neocortex. Synapse 1990; 5: 59–64.

18　Moody WJ. Control of spontaneous activity during development. J Neurobiol 1998; 37: 97–109.

19　Hodgkin AL, Huxley AF, Katz B. Measurement of current-voltage relations in the membrane of the giant axon of Loligo. J Physiol 1952; 116: 424–48.

20　Engel D, Jonas P. Presynaptic action potential amplification by voltage-gated Na^+ channels in hippocampal mossy fiber boutons. Neuron 2005; 45: 405–17.

21　Yost CS. Potassium channels: basic aspects, functional roles, and medical significance. Anesthesiology 1999; 90: 1186–203.

22　Banker GA, Cowan WM. Rat hippocampal neurons in dispersed cell culture. Brain Res 1977; 126: 397–42.

23　Bartlett WP, Banker GA. An electron microscopic study of the development of axons and dendrites by hippocampal neurons in culture. II. Synaptic relationships. J Neurosci 1984; 4: 1954–65.

24　Benson DL, Watkins FH, Steward O, Banker G. Characterization of GABAergic neurons in hippocampal cell cultures. J Neurocytol 1994; 23: 279–95.

25　Li L, Tao HY, Chen JB. Anti-apoptosis effect of astragaloside on adriamycin induced rat's cardiotoxicity. Zhongguo Zhong Xi Yi Jie He Za Zhi 2006; 26: 1011–4. Chinese

26　Marszalec W, Song JH and Narahashi T. The effects of the muscle relaxant, CS-722, on synaptic activity of cultured neurons. Br J Pharmacol 1996; 119: 126–32.

27　Gu Y, Wang G, Pan G, Fawcett JP, A J, Sun J. Transport and bioavailability studies of astragaloside IV, an active ingredient in Radix Astragali. Basic Clin Pharmacol Toxicol 2004; 95: 295–8.

28　Huang CR, Wang GJ, Wu XL, Li H, Xie HT, Lv H, *et al*. Absorption enhancement study of astragaloside IV based on its transport mechanism in caco-2 cells. Eur J Drug Metab Pharmacokinet 2006; 31: 5–10.

29　Choi DW. Calcium-mediated neurotoxicity: relationship to specific channel types and role in ischemic damage. Trends Neurosci 1988; 11: 465–9.

30　Rothman SM, Olney JW. Glutamate and the pathophysiology of hypoxic-ischemic brain damage. Ann Neurol 1986; 19: 105–11.

31　Goldin SM, Subbarao K, Sharma R, Knapp AG, Fischer JB, Daly D, *et al*. Neuroprotective use-dependent blockers of Na^+ and Ca^{2+} channels controlling presynaptic release of glutamate. Ann N Y Acad Sci 1995; 765: 210–29.

32　Taylor CP, Meldrum BS. Na^+ channels as targets for neuroprotective drugs. Trends Pharmacol Sci 1995; 16: 309–16.

33　Lee JM, Zipfel GJ, Choi DW. The changing landscape of ischaemic brain injury mechanisms. Nature 1999; 399: A7–14.